

# Mutation Causing Self-Aggregation in Human $\gamma$ C-Crystallin Leading to Congenital Cataract

Venu Talla,<sup>1</sup> Chitra Narayanan,<sup>2</sup> Narayanaswamy Srinivasan,<sup>2</sup>  
and Dorairajan Balasubramanian<sup>1</sup>

**PURPOSE.** Many forms of congenital hereditary cataract are associated with mutations in the crystallin genes. The authors focus attention on congenital lamellar cataract, which is associated with the R168W mutation in  $\gamma$ C-crystallin, and congenital zonular pulverulent cataract, which is associated with a 5-bp insertion in the  $\gamma$ C-crystallin gene.

**METHODS.** To understand the molecular phenotypes—i.e., the functional defects that have occurred in the mutant  $\gamma$ C-crystallin molecule in two cases described—the authors cloned, expressed, isolated, and compared the solution state structural features of these mutants with those of normal (wild-type)  $\gamma$ C-crystallin. Structural models of the wild-type and mutant have been generated using comparative modeling. Circular dichroism and fluorescence spectroscopic methods were used to determine the conformation of the proteins, and temperature dependent self-aggregation was used to observe the quaternary structural features. The structural stability of the proteins was monitored with the use of chemical and thermal denaturation.

**RESULTS.** The authors found that the 5-bp insertion led to a loss of secondary and tertiary structures of the molecule and to an enhanced tendency of self-aggregation into light-scattering particles, offering a possible factor in lens opacification. The R168W mutant, on the other hand, was remarkably similar to the wild-type molecule in its conformation and structural stability, but it differed in its ability to aggregate and scatter light.

**CONCLUSIONS.** These results support the idea that unfolding or structural destabilization is not always necessary for crystallin-associated cataractogenesis. (*Invest Ophthalmol Vis Sci.* 2006; 47:5212–5217) DOI:10.1167/iovs.06-0427

Cataract, or lens opacification, is a widespread eye disease that particularly affects the elderly. A host of risk factors have been identified, prominent among which are oxidative stress, diabetes, high levels of solar radiation, smoke inhalation, and nutritional deficiencies.<sup>1,2</sup> In contrast to age-related forms

of cataract, congenital cataracts that are present at birth or that develop in early childhood are less well studied. Worldwide every year an estimated 200,000 children are born blind with bilateral cataract, and 20,000 to 40,000 are born with developmental cataract.<sup>3</sup> In southern India, the prevalence of congenital cataract is estimated to be 1 to 4 cases per 10,000 children examined.<sup>4</sup> A major portion of these is hereditary, or genetic, in origin.

Studies on congenital hereditary cataract<sup>5</sup> have implicated a variety of lens membrane proteins, transcription factors, and major structural proteins of the lens cytosol, namely the soluble  $\alpha$ -,  $\beta$ -, and  $\gamma$ -crystallins (which constitute approximately 40% of the lens weight; most of the remaining weight is from water). Study of the mutations in the cytosolic proteins, such as the crystallins, is of interest and convenience because it would be possible to clone, express, and isolate the mutant proteins and compare their conformational and other properties with those of the normal (wild-type) molecules. Such a comparison is expected to provide some insight into the molecular phenotypic aspects of lens opacification. Indeed, it has been possible to obtain information of this kind with, for example, some mutant forms of  $\alpha$ -crystallin,<sup>6</sup>  $\beta$ B<sub>1</sub>-crystallin,<sup>7</sup>  $\beta$ A<sub>3</sub>/A<sub>1</sub>-crystallin,<sup>8</sup>  $\gamma$ B-crystallin,<sup>9</sup>  $\gamma$ C-crystallin,<sup>10</sup> and  $\gamma$ D-crystallin,<sup>11–14</sup> which are associated with various forms of congenital hereditary cataract.

We report our results on the study of conformational and related properties of two mutant  $\gamma$ C-crystallins. The first is a 5-bp duplication (5-bp dup) within exon 2 of  $\gamma$ C-crystallin, which disrupts the reading frame of the coding sequence. In this case, it appears that if the transcribed mRNA escapes the usual nonsense-mediated decay (NMD) quality control mechanism and is translated, the resultant mutant protein would be altered in its structure and, thus, associated with cataract. This mutant protein is expected to preserve the N-terminal 38 residues in the first “Greek key” motif, followed by approximately 70 random amino acids. Indeed, this mutation is associated with autosomal dominant variable zonular pulverulent cataract.<sup>15</sup> The second is the mutation R168W, arising out of a point mutation in exon 3 (502 C→T) in the gene. The resultant protein would contain the replacement of a charged residue by a hydrophobic aromatic one and thus would be expected to have a structural perturbation. It has been suggested that this mutation is associated with congenital lamellar cataract.<sup>16</sup>

## MATERIALS AND METHODS

### Expression and Purification of Recombinant Proteins

**Cloning of Wild-Type  $\gamma$ C and 5-bp dup Variant.** cDNAs of mutant and wild-type  $\gamma$ C-crystallin cloned into pET20b(+) were amplified with Pfu DNA polymerase using the forward primer (5'-GC[UNDERLN]GGATCC[UNDERLN]GGGAAGATCACCTTCT-3') and the reverse primer (5'-GC[UNDERLN]CTCGAG[UNDERLN]TAATACAAATCCACCACTCT-3'), which harbor the restriction sites for *Bam*HI and *Xba*I, respectively (as underlined in the sequence). PCR products were cloned into the *Sma*I site of pBSSK vector. Nucleotide

From the <sup>1</sup>Brien Holden Eye Research Centre, L. V. Prasad Eye Institute, Hyderabad, India; and the <sup>2</sup>Molecular Biophysics Unit, Indian Institute of Science, Bangalore, India.

Supported by grants from the Department of Science & Technology, Government of India, and the Wellcome Trust (NS). TV is the recipient of a Senior Research Fellowship of the Council of Scientific and Industrial Research, India. DB is a Visiting Professor at the University of New South Wales, Sydney, Australia; a Senior Fellow of the University of Melbourne, Australia; and an Adjunct Professor at the Birla Institute of Technology and Science, Pilani, India.

Submitted for publication April 15, 2006; revised July 1 and August 3, 2006; accepted October 11, 2006.

Disclosure: V. Talla, None; C. Narayanan, None; N. Srinivasan, None; D. Balasubramanian, None

The publication costs of this article were defrayed in part by page charge payment. This article must therefore be marked “advertisement” in accordance with 18 U.S.C. §1734 solely to indicate this fact.

Corresponding author: Dorairajan Balasubramanian, Brien Holden Eye Research Centre, L. V. Prasad Eye Institute, L. V. Prasad Marg, Banjara Hills, Hyderabad 500 034, India; dbala@lvpei.org.

sequences of the wild-type and 5-bp dup  $\gamma$ C-crystallins were verified by sequencing (ABI 3700 automated DNA sequencer; Applied Biosystems, Foster City, CA) with pBSSK vector-specific T3 and T7 primers. The inserts were released from the pBSSK vector by restriction digestion with *Bam*H1/*Xba*I and were subcloned into the *Bam*H1 and *Xba*I sites of PGEX 5X-3 vector.

**Cloning of Wild-Type  $\gamma$ C-Crystallin and R168W Variant of  $\gamma$ C-Crystallin.** The cDNA of wild-type  $\gamma$ C-crystallin was amplified by Pfu DNA polymerase using the forward primer (5'-GGAAATTC[UNDERLN]CATATG[UNDERLN]GGGAAGATCACCTTCT-3') and the reverse primer (5'-CCC[UNDERLN]AAGCTT[UNDERLN]TTAATACAAATCCACCCTCT-3'). The mutant R168W cDNA was amplified by the forward and reverse primers with the incorporated single base at the 3' end, as shown in bold in the primer sequence 5'-C[UNDERLN]AAGCTT[UNDERLN]TTAATACAAATCCACCCTCT-CC[b]AC-3'. Forward primers harbored the *Nde*I site, and reverse primers harbored the *Hind*III site (as underlined in the primer sequence). PCR products were cloned into the *Sma*I site of the pBSSK vector. Nucleotide sequences of the wild-type and R168W mutant  $\gamma$ C-crystallins were verified by sequencing (ABI 3700 automated DNA sequencer; Applied Biosystems) with pBSSK vector-specific T3 and T7 primers. Inserts were released from pBSSK by restriction digestion with *Nde*I/*Hind*III and subcloned into *Nde*I/*Hind*III sites of pET21a(+) vector.

### Purification of Recombinant Proteins

For the overexpression of the wild-type, 5-bp dup  $\gamma$ C, and R168W  $\gamma$ C-crystallins, *Escherichia coli* strain BL21 (DE3) pLysS was transformed with the expression constructs pGEX-WT  $\gamma$ C, pGEX 5-bp dup  $\gamma$ C, pET-WT  $\gamma$ C, and pET-R168W  $\gamma$ C. Gene expression and protein purification methods were as described elsewhere.<sup>17</sup> The recombinant proteins expressed from pGEX 5x-3 were purified from the supernatant by glutathione-S-transferase (GST) affinity chromatography. Purified GST fusion proteins were subjected to factor Xa digestion for 16 hours, and factor Xa and GST were removed by passing the protein solution through benzamidine Sepharose-4B and glutathione Sepharose-4B columns, respectively. Purity of the recombinant proteins was confirmed by SDS-PAGE. Protein concentrations were determined by measuring the absorbance at 280 nm. The R168W and wild-type  $\gamma$ C-crystallin protein preparations were stored in 50 mM Tris-Cl, pH 7.4, and the 5-bp dup mutant and wild-type  $\gamma$ C-crystallin proteins were stored in 10 mM PBS (phosphate-buffered saline) at 4°C.

### Spectroscopic Analysis of the Proteins in Solution

Intrinsic fluorescence spectra were recorded using a fluorescence spectrophotometer (F-2500; Hitachi, Tokyo, Japan) with an excitation wavelength of 295 nm and the emission range of 300 to 400 nm. Excitation and emission slits were set at 2.5 nm. Three scans of each spectrum were averaged and smoothed, and baselines (of buffer alone) were subtracted. Spectra using the extrinsic probe 8-anilinonaphthalene-1-sulfonate (ANS) were recorded by adding 100  $\mu$ M ANS to a 0.1-mg/mL solution of the protein, exciting at 390 nm, and recording the emission wavelength and intensity in the 500-nm range.<sup>18</sup> Circular dichroism (CD) spectra were recorded with a spectropolarimeter (J-715; Jasco, Easton, MD) at room temperature. Protein concentrations of 0.6 mg/mL and 0.1 mg/mL were used for recording the near and far ultraviolet (UV) CD spectra with 1-cm and 0.1-cm path-length quartz cells, respectively. Three scans of each spectrum were averaged and smoothed, and baselines (of buffer) were subtracted.

### Thermal Stability Measurements

For time-dependent scattering measurements, the fluorescence spectrophotometer was used, excitation and emission wavelengths were set at 400 nm, and measurements were performed at 65°C. Solutions of the wild-type and mutant proteins, each at 0.1 mg/mL in Tris buffer, were taken, and the scattering at 400 nm was measured as a function of time, up to 900 seconds. Thermal denaturation of the wild-type and

mutant proteins was followed by monitoring of the temperature-dependent changes in the Trp emission intensity (excitation at 295 nm) and wavelength, measured at 5°C intervals between 20° and 70°C. A 20-minute equilibrium time was allowed for each temperature change, and the temperature was controlled with a water bath (F-12; Julabo Labortechnik GmbH, Seelbach, Germany). Chemical denaturation studies were performed with a 6-M stock solution of guanidine hydrochloride (Gdn.HCl) in 50 mM Tris-Cl buffer, pH 7.4. Protein samples were diluted into a range of concentrations of Gdn.HCl from 0 to 6 M and with a protein concentration of 0.1 mg/mL. Samples were equilibrated overnight at room temperature. Fluorescence spectra were obtained using spectrofluorometer (F-2500; Hitachi) equipped with a thermostatically controlled circulating water bath and an excitation wavelength of 295 nm. Excitation and emission slits were set to 2.5 nm, and emission spectra were collected from 300 to 400 nm with the use of a 1-cm path-length cell. Baseline spectra of Gdn.HCl solutions from 0 to 6 M were subtracted, and the emission intensity at 320 nm was used for data analysis.

### Computer Analysis

**Sequence-Based Search.** The sequence of  $\gamma$ C-crystallin was queried against the nonredundant database (NRDB) using a position-specific search strategy called PSI-BLAST,<sup>19</sup> with an E-value cutoff of 0.001 to identify all the related proteins based on sequence similarity. The Hidden Markov Model (HMM)-based search, HMMPfam,<sup>20</sup> was also performed against the Pfam database<sup>21</sup> to assign Pfam domains to this protein.

**Structure-Based Search.** The sequence of  $\gamma$ C-crystallin was submitted to the different fold recognition servers, including FUGUE<sup>22,23</sup> and position-specific scoring matrix, or 3D-PSSM,<sup>24</sup> to identify homologues based on sequence-structure comparison. A hit obtained with high reliability, determined by the score corresponding to each one, was used as a template to generate the structure of this protein. The template identified corresponded to the crystal structure of bovine  $\gamma$ B-crystallin mutant, which corresponded to the protein databank code 1I51.

**Comparative Modeling of  $\gamma$ C-Crystallins.** The three-dimensional structure of  $\gamma$ C-crystallin was modeled on the basis of the crystal structure of bovine  $\gamma$ B-crystallin mutant. The structure was generated using homology modeling software (MODELLER,<sup>25</sup> version 7). The generated structure was energy minimized using a computational toolkit (SYBYL; Tripos, Inc., St. Louis, MO) to remove short contacts and to optimize the stereochemistry of the molecule. Minimization was performed in SYBYL using the standard AMBER force field, as described.<sup>26</sup> The charges of the atoms used during the course of minimization are exactly the same as prescribed in the standard AMBER protocol.<sup>26</sup> During the initial cycles of energy minimization, the backbone was kept rigid and side chains alone were moved. Subsequently, all atoms in the structure were allowed to move during minimization. Energy minimization was performed until all short contacts and inconsistencies in geometry were rectified. During the initial stages of minimization, the electrostatic term was not included because the main objective was to relieve steric clashes and to rectify bad geometry. In the later cycles of energy minimization, the electrostatic term was included with the distance-dependent dielectric constant. Energy minimization steps involved the use of a simplex method in the initial rounds of minimization and later the Powell algorithm. GRASP<sup>27</sup> was used to study the distribution of charge on the electrostatic surface potential of the protein.

**Mutant Generation.** The structure of the mutant was generated by replacing the arginine residue at position 168 with tryptophan (R168W) in the MODELLER-generated structure of  $\gamma$ C-crystallin. The mutant structure thus obtained was optimized by energy minimization in SYBYL using the AMBER force field, as described. The surface charge distribution of the mutant structure was determined using GRASP. The GRASP outputs of wild-type and mutant structures were analyzed to study the possible structural and surface changes in the mutant structure, leading to the enhanced aggregation of the mutant protein.

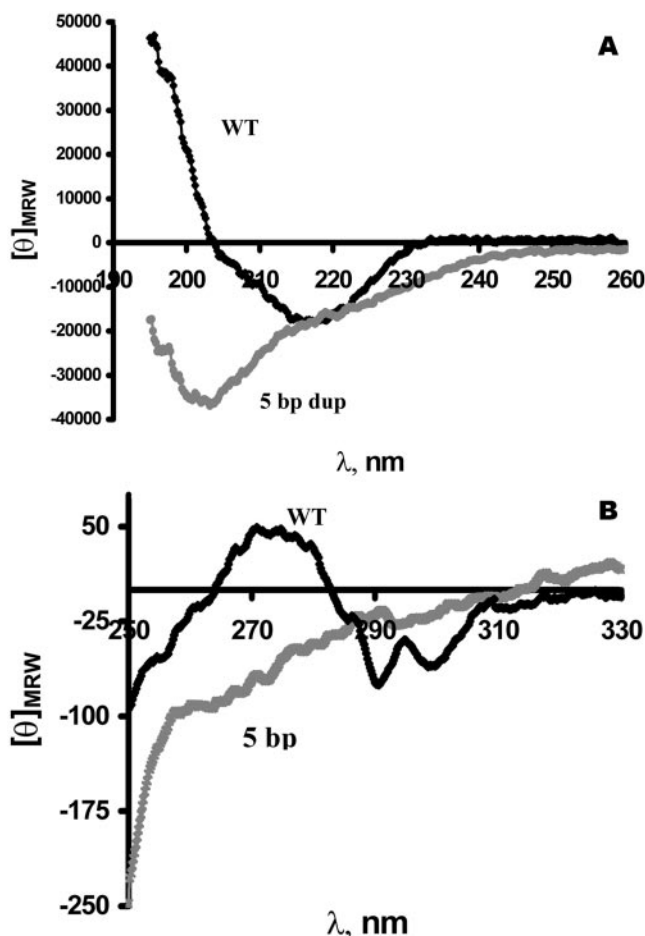


FIGURE 1. (A) Far UV CD spectra of the wild-type (WT) and 5-bp dup mutant human  $\gamma$ C-crystallin. Ellipticity values are expressed in residue molar units. (B) Near UV CD spectra of the WT and 5-bp dup mutant human  $\gamma$ C-crystallin.

## RESULTS

### 5-bp Insertion Mutant Protein: Modeling and Spectral Analysis

Repetition of the 5-bp sequence GCGGC at positions 226 to 230 within exon 2 of the  $\gamma$ C-crystallin gene disrupted the reading frame. The resultant protein maintained homology only in the N-terminal 38 residue sequence of the first Greek key motif with the wild-type molecule. This homologous sequence was followed in the mutant by a much longer sequence of random amino acids. Computer modeling of the chain conformation of this mutant sequence revealed that the N-terminal 38 residues represented the first half of the first domain of the canonical two-domain structure characteristic of the  $\gamma$ -crystallins. The other half of the first domain was a structural repeat of the first half. Considering all known structures of the crystallins and related systems, we inferred that there was no evidence that the first half of the first domain (i.e., the N-terminal 38-residue sequence) had a stable structure of its own. In addition, the amino acid sequence of the latter part of the mutant molecule suggested no ordered structure. We expected this mutant  $\gamma$ C-crystallin molecule to exist in a disordered chain conformation.

Spectroscopic study of the protein, shown in Figure 1, supported this prediction. The far UV CD spectrum corresponded to that of a random coil, and the near UV spectrum

also showed no tertiary structural order. The intrinsic fluorescence of the protein, largely because of its Trp residues, showed a band maximum at 340 nm, red shifted by 14 nm from that of the wild-type molecule (Fig. 2, top). Surface hydrophobicity of the mutant was evaluated with the fluorescence spectrum of the extrinsic probe ANS. The 20-nm blue shift and threefold enhanced intensity of the probe bound to the mutant—in contrast to when it bound to the wild-type molecule (Fig. 2, bottom)—indicated that the mutant molecule had a more pronounced hydrophobic surface.<sup>18</sup> We further noted that the protein was soluble only at concentrations lower than 0.1 mg/mL. When the concentration was increased to at least 0.3 mg/mL, the protein coagulated and dropped out of solution.

### Solution State Studies of the R168W Mutant

This mutation involved the replacement of an otherwise highly conserved Arg residue at position 168 by Trp, in the fourth Greek key motif of  $\gamma$ C-crystallin. Figure 3A shows that the fluorescence emission of the mutant was red-shifted by 14 nm compared with that of the wild-type (340 nm, cf. 326 nm) and that its intensity was enhanced. Both these features indicated the Trp residues to experience a more polar environment in the mutant. Extrinsic fluorescence studies, using the apolar reporter ANS, showed a modest enhancement in the emission intensity of the probe bound to the R168W mutant, in contrast to when it was bound to the wild-type protein (Fig. 3B).

Figure 4 shows the guanidinium chloride-induced denaturation and thermal denaturation curves of the wild-type and R168W  $\gamma$ C-crystallins. Little difference was observed between

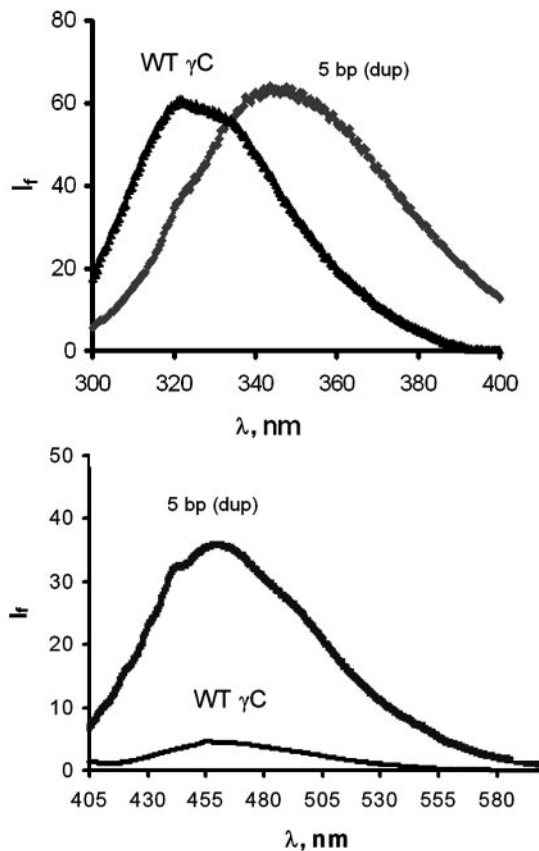
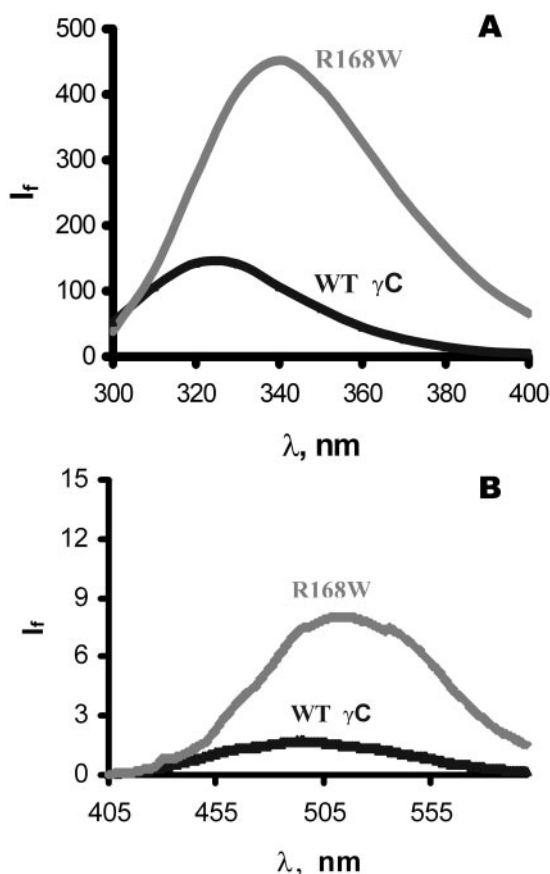


FIGURE 2. Top: intrinsic fluorescence of wild-type and 5-bp dup mutant human  $\gamma$ C-crystallin. Excitation at 295 nm. Bottom: extrinsic fluorescence of the surface hydrophobicity probe ANS bound to WT and 5-bp dup human  $\gamma$ C-crystallin. Excitation at 390 nm.



**FIGURE 3.** (A) Intrinsic fluorescence of wild-type and R168W human  $\gamma$ C-crystallin. Excitation at 295 nm. (B) Extrinsic fluorescence of the surface hydrophobicity probe ANS bound to WT and R168W human  $\gamma$ C-crystallin. Excitation at 390 nm.

the two, indicating that the structural stability of the molecule was not altered much by the replacement of the Arg residue at this position by Trp. Figure 5A compares the far UV CD spectra and reveals that the mutation did not affect the secondary structure or backbone conformation of the molecule. Figure 5B, which compares the tertiary structural features revealed by near UV CD spectroscopy, shows some minor differences that might have come about near the aromatic side chain molecule with the replacement of R168 by W.

An interesting property of  $\gamma$ -crystallin solutions, thought to be relevant to the opacification of the eye lens, is their tendency on heating to produce self-aggregates, of submicrometer size, that scatter light.<sup>28-30</sup> This property has enabled  $\gamma$ -crystallins to be used as target proteins to evaluate the solubilizing ability, or the chaperone-like action, of lens  $\alpha$ -crystallin.<sup>31,32</sup> We thus decided to compare the thermally induced light scattering of wild-type and R168W  $\gamma$ C-crystallins. Figure 6 reveals that at 65°C the light-scattering intensity of the mutant increased eightfold within 15 minutes, whereas that of the wild-type protein increased only twofold. It took approximately 30 minutes for the wild-type protein solution to increase its light scattering eightfold, by which time the mutant protein precipitated out of solution.

#### R168W Mutant: Modeling Studies

The HMM based search of the  $\gamma$ C-crystallin sequence against the Pfam database led to the identification of two domains, both corresponding to the  $\beta\gamma$ -crystallin family of proteins ( $E = 8.8 \times 10^{-47}$  and  $E = 2.2 \times 10^{-49}$ , respectively). The query

picked up homologous  $\gamma$ -crystallin proteins as hits with high reliability in the PSI-BLAST search against the NRDB. Several  $\gamma$ -crystallins, whose crystal structures have been determined, were picked up with high sequence identities of approximately 75%. The structure-based search using the different fold recognition servers led to the identification of several  $\gamma$ -crystallins with high reliability (FUGUE Z score  $>6.0$ ). The top hit with the highest score, a bovine  $\gamma$ B-crystallin mutant<sup>9</sup> (protein databank code, 1I5D), shared 75% identity with the human  $\gamma$ C-crystallin. Therefore, the structure of this protein was used as a template to generate the model of the human  $\gamma$ C-crystallin.

$\gamma$ -Crystallins are known to be composed of two similar domains folded into a Greek key motif pattern, each of which, in turn, is composed of two similar motifs. The two domains are connected by a short loop region. The R168W mutant structure was expected to retain the overall fold of the wild-type because the site of mutation was solvent exposed and the modeled structure confirmed that Trp in the mutant was accommodated comfortably in the classic  $\gamma$ -crystallin fold. This Trp168 residue was observed to be solvent accessible with the nitrogen atom of the side chain toward the exterior, suggesting a possible polar interaction of the Trp side chain.

In the wild-type model, the Arg side chain was seen to form hydrogen bonds within the domain in which it was situated. No strong interaction was seen between the Arg side chain and the other domain across the domain-domain interface. In the mutant structure, Trp was exposed because of the lack of sufficient space between the two domains of crystallin fold (Fig. 7A). The three-dimensional model of the molecule showed a good number of exposed aromatic side chains, positively charged side chains, and Cys and Met residues, all of

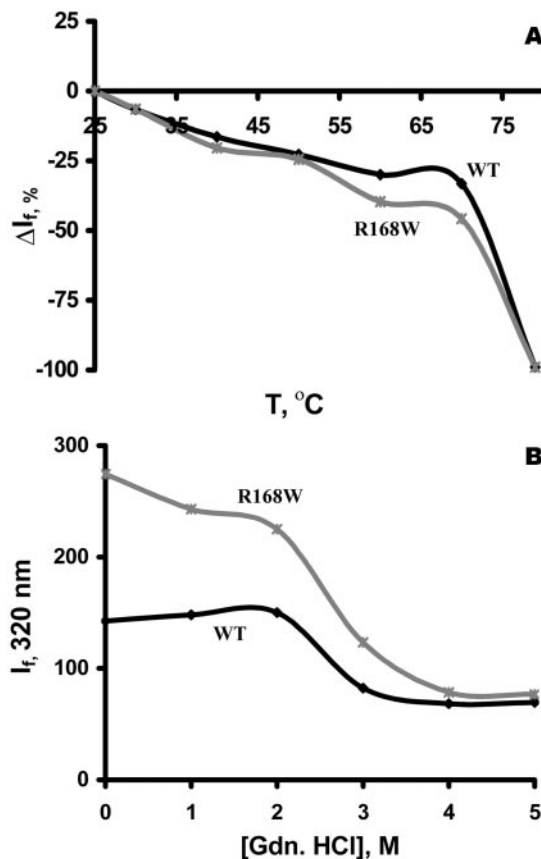


**FIGURE 4.** Comparison of the thermal (A) and Gdn.HCl-induced (B) denaturation profiles of wild-type (WT) and R168W human  $\gamma$ C-crystallin. Denaturation was monitored using Trp fluorescence.

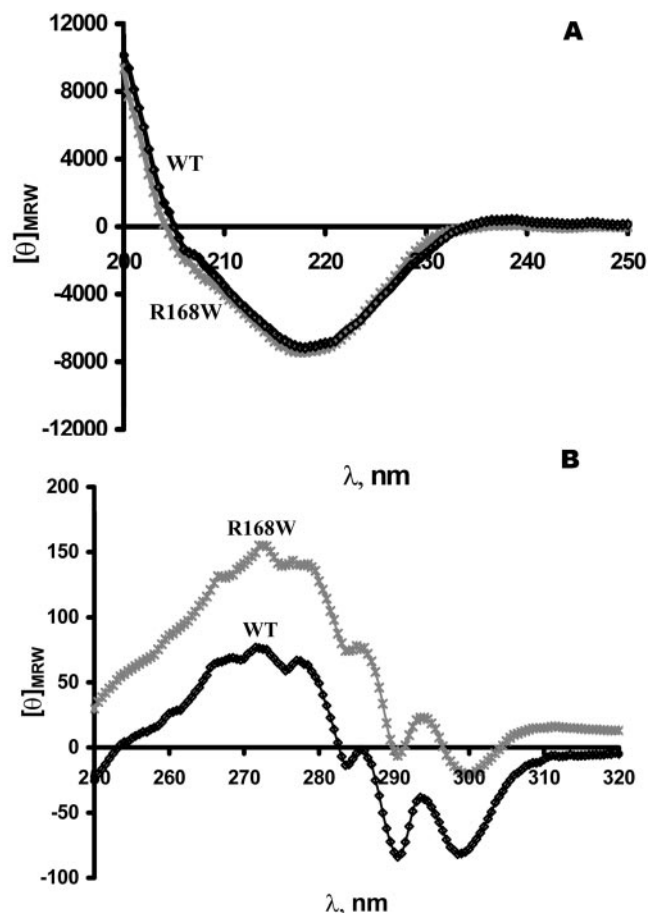


FIGURE 5. Far UV CD (A) and near UV CD (B) spectra of wild-type (WT) and R168W human  $\gamma$ C-crystallin.

which were capable of interacting with the exposed Trp in the site of mutation (Fig. 7B). The overall solvent accessible surface areas of Arg (in the wild type) and Trp (in the mutant) in the modeled structures were  $11.3\text{\AA}^2$  and  $12.5\text{\AA}^2$ , respectively. Although this overall difference in accessible surface area was not prominent, the accessible surface areas contributed by hydrophobic surface of Arg and Trp measured  $2.7\text{\AA}^2$  and  $9\text{\AA}^2$ ,

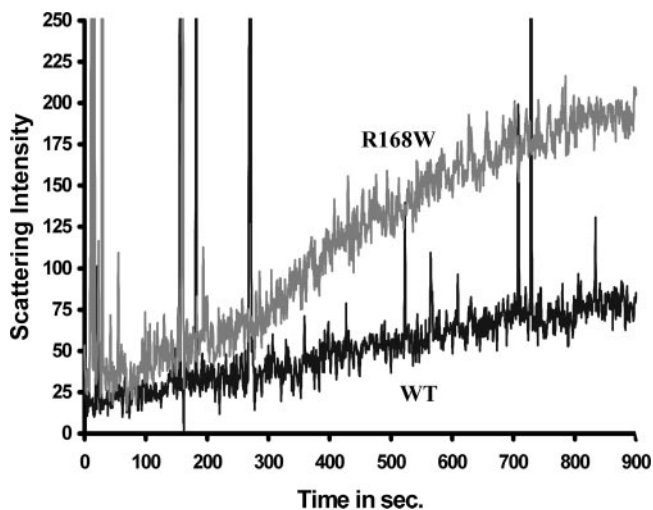


FIGURE 6. Thermal aggregation profiles of wild-type (WT) and R168W human  $\gamma$ C-crystallin.

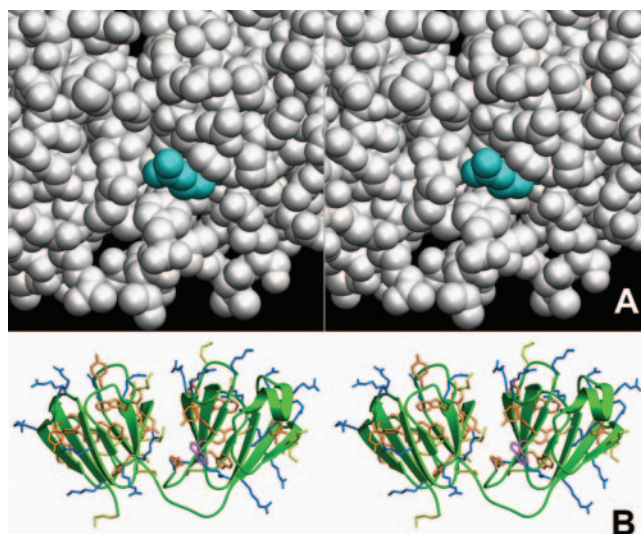


FIGURE 7. (A) Stereo pair of the close-up of the interdomain interface in the R168W mutant model, with the Trp at the site of mutation *highlighted*. This Trp residue was exposed because of lack of sufficient space in the domain-domain interface; this feature might contribute to aggregation. The image was produced with the three-dimensional model representation SETOR. (B) Stereo pair of the modeled structure of the R168W mutant. Aromatic, basic (cationic), and sulfur-containing residues are shown in different colors. Many of these residues are exposed. The Trp at the site of mutation is *highlighted in pink*. This figure was produced with SETOR.

respectively. Thus, in the tertiary structure of the mutant compared with wild type, there was a substantial increase ( $6.3\text{\AA}^2$ ) in the hydrophobic surface. These features provided a possible explanation of the faster aggregation rate of the mutant structure compared with the wild-type human  $\gamma$ C-crystallin. The surface charge distribution data, obtained with the use of GRASP, did not show any significant changes in the charge distribution on the surface of the wild-type and mutant  $\gamma$ -crystallins.

## DISCUSSION

The 5-bp mutant of  $\gamma$ C-crystallin did, as shown, lose much of the chain conformation, and it exhibited reduced solubility. Surface probe studies revealed this molecule to have a noticeable hydrophobic surface, which might have been related to its lower solubility and greater tendency to self-aggregate. These features of conformational loss and increased tendency to self-aggregate were in contrast to those of wild-type  $\gamma$ C-crystallin and provided a molecular phenotypic explanation of its association with congenital cataract.

It is, however, the case of the R168W that is unusual. Its chain conformation and tertiary structure, as revealed by spectroscopy, were not very different from the wild-type molecule. Modeling studies showed subtle variations in the side chain interactions that were not reflected as major changes in tertiary structure or in structural stability. They seem reflected more in terms of aggregation and precipitation properties. In this regard, the behavior of R168W was reminiscent of that of two other cataract-associated crystallin mutants, R14C and R58H human  $\gamma$ D-crystallins, studied by Pande et al.<sup>11,12</sup> These two mutants displayed essentially the same secondary and tertiary structures and the same stability regarding thermal unfolding, but they aggregated and precipitated more readily than wild-type  $\gamma$ D-crystallin. Pande et al.<sup>11,12</sup> suggested that it is the self-aggregation, or quaternary, structural difference that is

responsible for the phenotypic association with lens opacification or cataractogenesis. Our results support this hypothesis.

Many genetic cataracts are associated with mutation of the Arg residue of crystallins.<sup>33-35</sup> The Arg residue, as our results from modeling analysis show, is in extensive contact with other residues and with solvent water. Substitution with another residue appears to disturb this networking, altering the quaternary structure in turn. This has been clarified by the crystal structural comparison of wild-type  $\gamma$ D-crystallin with its R58H mutant.<sup>14</sup> In the present study, too, substitution of Arg by Trp resulted in a marked increase in the exposed hydrophobic surface in the tertiary structure, consistent with the observation of aggregation. That such behavior is not limited to Arg mutants alone has recently been shown by Evans et al.<sup>36</sup> and Pande et al.<sup>13</sup> with regard to the P23T mutant of  $\gamma$ D-crystallin, which self-aggregates more readily than the wild-type molecule. Hence, it appears that unfolding or destabilization of the crystallins is not always necessary for them to generate lens opacification.

### Acknowledgments

The authors thank Yogendra Sharma of the Centre for Cellular and Molecular Biology, Hyderabad, India, for ready help and advice with the cloning experiments.

### References

- McCarty CA, Nanjan MB, Taylor HR. Attributable risk estimates for cataract to prioritize medical and public health action. *Invest Ophthalmol Vis Sci.* 2000;41:3720-3725.
- Balasubramanian D. Photodynamics of cataract: an update on endogenous chromophores and antioxidants. *Photochem Photobiol.* 2005;81:498-501.
- Foster A, Gilbert C, Rahi J. Epidemiology of cataract in childhood: a global perspective. *J Cataract Refract Surg.* 1997;23:601-604.
- Dandona L, Williams JD, Williams BC, Rao GN. Population based assessment of childhood blindness in Southern India. *Arch Ophthalmol.* 1998;116:545-546.
- Graw J. Congenital hereditary cataracts. *Int J Dev Biol.* 2004;48:1031-1044.
- Kumar LV, Ramakrishna T, Rao CM. Structural and functional consequences of the mutation of a conserved arginine residue in  $\alpha$ A and  $\alpha$ B crystallins. *J Biol Chem.* 1999;274:24137-24141.
- Annunziata O, Pande A, Pande J, Ogun O, Lubsen NH, Benedek GB. Oligomerization and phase transitions in aqueous solutions of native and truncated human beta B1-crystallin. *Biochemistry.* 2005;44:1316-1328.
- Kannabiran C, Rogan PK, Olmos L, et al. Autosomal dominant zonular cataract with sutural opacities is associated with a splice mutation in the betaA3/A1-crystallin gene (review). *Mol Vis.* 1998;23:21.
- Asherie N, Pande J, Pande A, et al. Enhanced crystallization of the Cys18 to Ser mutant of bovine  $\gamma$ B crystallin. *J Mol Biol.* 2001;314:663-669.
- Fu L, Liang JN. Conformational change and destabilization of cataract  $\gamma$ C-crystallin T5P mutant. *FEBS Lett.* 2002;513:213-216.
- Pande A, Pande J, Asherie N, et al. Molecular basis of a progressive juvenile-onset hereditary cataract. *Proc Natl Acad Sci USA.* 2000;97:993-1998.
- Pande A, Pande J, Asherie N, et al. Crystal cataracts: human genetic cataract caused by protein crystallization. *Proc Natl Acad Sci USA.* 2001;98:6116-6120.
- Pande A, Annunziata O, Asherie N, Ogun O, Benedek GB, Pande J. Decrease in protein solubility and cataract formation caused by the Pro23 to Thr mutation in human gamma D-crystallin. *Biochemistry.* 2005;44:2491-2500.
- Basak A, Bateman O, Slingsby C, et al. High-resolution X-ray crystal structures of human  $\gamma$ D crystallin (1.25 Å) and the R58H mutant (1.15 Å) associated with aculeiform cataract. *J Mol Biol.* 2003;328:1137-1147.
- Ren Z, Li A, Shastry BS, et al. A 5-base insertion in the  $\gamma$ C-crystallin gene is associated with autosomal dominant variable zonular pulverulent cataract. *Hum Genet.* 2000;106:531-537.
- Santhiya ST, Shyam Manohar M, Rawley D, et al. Novel mutations in the  $\gamma$ -crystallin genes cause autosomal dominant congenital cataracts. *J Med Genet.* 2002;39:352-358.
- Sun T-X, Das BK, Liang JJ-N. Conformational and functional differences between recombinant human lens  $\alpha$ A- and  $\alpha$ B-crystallins. *J Biol Chem.* 1997;272:6220-6225.
- Cardamone M, Puri NK. Spectrofluorometric assessment of the surface hydrophobicity of proteins. *Biochem J.* 1992;282:589-593.
- Altschul SF, Madden TL, Schaffer AA, et al. Gapped and PSI-BLAST: a new generation of protein database search program. *Nucleic Acids Res.* 1997;25:3389-3402.
- Eddy SR. Profile hidden Markov models. *Bioinformatics.* 1998;14:755-763.
- Bateman A, Birney E, Durbin R, Eddy SR, Howe KL, Sonnhammer EL. The Pfam protein families database. *Nucleic Acids Res.* 2000;28:263-266.
- Shi J, Blundell TL, Mizuguchi K. FUGUE: sequence-structure homology recognition using environment-specific substitution tables and structure-dependent gap penalties. *J Mol Biol.* 2001;310:243-257.
- Mizuguchi K, Deane CM, Blundell TL, Johnson MS, Overington JP. JOY: protein sequence-structure representation and analysis. *Bioinformatics.* 1998;14:617-623.
- Kelly LA, Maccallum R, Sternberg MJE. Recognition of remote homologies using three-dimensional information to generate a position-specific scoring matrix in the program 3D-PSSM. *RECOMB 99. Proceedings of the Third Annual Conference on Computational Molecular Biology.* 1999;218-225.
- Sali A, Blundell TL. Comparative protein modeling by satisfaction of spatial constraints. *J Mol Biol.* 1993;339:1103-1113.
- Weiner SJ, Kollmann PA, Case DA, et al. A new forcefield for molecular mechanical simulations of nucleic acids and proteins. *J Am Chem Soc.* 1984;106:765-784.
- Nicolls A, Sharp KA, Honig B. Protein folding and association: insights from the interfacial and thermodynamic properties of hydrocarbons. *Proteins Struct Funct Genet.* 1991;11:281-296.
- Raman B, Rao CM. Chaperone-like activity and quaternary structure of alpha crystalline. *J Biol Chem.* 1994;269:27264-27268.
- Kundu B, Shukla A, Guptasarma P. Peptide scanning-based identification of regions of gamma-II crystallin involved in thermal aggregation: evidence of the involvement of structurally analogous, helix-containing loops from the two double Greek key domains of the molecule. *Arch Biochem Biophys.* 2003;410:69-75.
- Mandal K, Kono M, Bose SK, Thomson J, Chakrabarti B. Structure and stability of gamma-crystallins, IV: aggregation and structural destabilization in photosensitized reactions. *Photochem Photobiol.* 1988;47:583-591.
- Horwitz J.  $\alpha$ -Crystallin can function as a molecular chaperone. *Proc Natl Acad Sci USA.* 1992;89:10449-10453.
- Liang JN. Interactions and chaperone function of  $\alpha$ A-crystallin with T5P  $\gamma$ C-crystallin mutant. *Protein Sci.* 2004;13:2476-2482.
- Heon E, Priston M, Schorderet DF, et al. The gamma-crystallins and human cataracts: a puzzle made clearer. *Am J Hum Genet.* 1999;65:1261-1267.
- Kmoch S, Brynda J, Asfaw B, et al. Link between a novel human  $\gamma$ D-crystallin allele and a unique cataract phenotype explained by protein crystallography. *Hum Mol Genet.* 2000;9:1779-1786.
- Stephan DA, Gillanders E, Vanderveen D, et al. Progressive juvenile-onset punctate cataracts caused by mutation of the  $\gamma$ D-crystallin gene. *Proc Natl Acad Sci USA.* 1999;96:1008-1012.
- Evans P, Wyatt K, Wistow GJ, Bateman OA, Wallace BA, Slingsby C. The P23T cataract mutation causes loss of solubility of folded  $\gamma$ D-crystallin. *J Mol Biol.* 2004;343:435-444.